



PERGAMON

Available online at [www.sciencedirect.com](http://www.sciencedirect.com)

 ScienceDirect

Acta Astronautica 63 (2008) 1203–1214

ACTA  
ASTRONAUTICA

[www.elsevier.com/locate/actaastro](http://www.elsevier.com/locate/actaastro)

# Exploring the solar system galactic frontier in extreme ultraviolet

Mike Gruntman\*

*Aeronautics and Space Technology Division, USC Viterbi School of Engineering, 854 Downey Way, RRB-224, MC-1192, University of Southern California, Los Angeles, CA 90089-1192, USA*

Received 22 December 2006; received in revised form 18 June 2008; accepted 18 June 2008

Available online 14 July 2008

## Abstract

The solar system galactic frontier—the region where the expanding solar wind meets the surrounding galactic medium—remains poorly explored. The sheer size of the essentially asymmetric heliosphere calls for remote techniques to probe the properties of its global time-varying three-dimensional boundary. The Interstellar Boundary Explorer (IBEX) mission (launch in 2008) will image the region between the termination shock and the heliopause, the heliospheric sheath, in fluxes of energetic neutral atoms. Global imaging in extreme ultraviolet (EUV) will likely be the next logical step in remote exploration of the galactic frontier from 1 AU. Imaging in EUV will establish directional and spectral properties of (1) the glow of singly charged helium ( $\text{He}^+$ ) ions in the interstellar and solar wind plasmas; (2) emissions of hot plasma in the Local Bubble; and (3) characteristic emissions of the solar wind. Global imaging with ultrahigh sensitivity and ultrahigh spectral resolution will map the heliopause and reveal the three-dimensional flow pattern of the solar wind, including the flow over the Sun's poles. This article presents the emerging concept of the experiment and space mission for heliosphere global imaging in EUV.

© 2008 Elsevier Ltd. All rights reserved.

## 1. Galactic frontier

The interaction of the expanding solar wind plasma with the surrounding galactic medium—local interstellar medium (LISM)—creates the heliosphere [1–4]. The heliosphere is a complex phenomenon (Fig. 1) where the solar wind and interstellar plasmas, interstellar gas, magnetic field, and energetic particles all play important roles [5–8]. The region where the solar wind meets the galactic medium remains poorly explored. The most distant operating spacecraft, Voyager 1, had reached the termination shock and entered the slowed-down post-shock solar wind at 94 AU (ecliptic latitude  $\beta = 34.8^\circ$  and ecliptic longitude  $\lambda = 253.3^\circ$ ) in December 2004. Voyager 2 crossed the termination shock in September

2007 at 84 AU (ecliptic latitude  $\beta = -31.6^\circ$  and ecliptic longitude  $\lambda = 288.8^\circ$ ). In September 2008, Voyagers 1 and 2 are at heliocentric distances of 107.5 and 87.0 AU, respectively. Crossing the termination shock is a major milestone in exploration of the outer heliosphere, although Voyager spacecraft are instrumented for planetary flybys and not optimized for interstellar studies.

A possible Sun-LISM interaction [5] illustrates the main features of the heliosphere (Figs. 1 and 2). The interstellar wind (partially ionized interstellar gas) approaches the heliosphere with a supersonic velocity and forms a bow shock. Interstellar neutral atoms penetrate the heliosphere, some reaching the Sun's vicinity at 1 AU. The dynamic pressure of the expanding, highly supersonic solar wind decreases with the heliocentric distance. At a certain distance from the Sun, this pressure equals the external LISM pressure of the interstellar wind and magnetic field. The solar wind expansion

\* Tel.: +1 213 740 5536; fax: +1 213 821 5819.

E-mail address: [mikeg@usc.edu](mailto:mikeg@usc.edu).

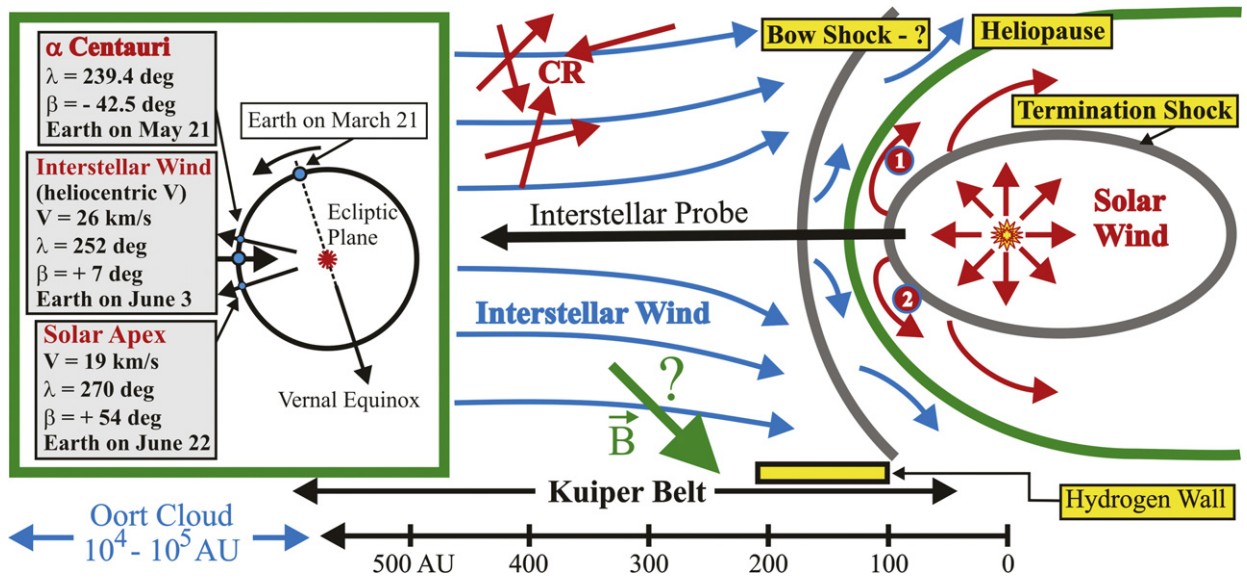


Fig. 1. Sun's galactic neighborhood. The interaction of the expanding solar wind with the surrounding interstellar medium creates the heliosphere; CR—cosmic rays; B—interstellar magnetic field. Circles 1 and 2 show positions of Voyagers 1 and 2 spacecraft, respectively, heading in antisolar directions. The future Interstellar Probe will fly in the upwind (with respect to the interstellar wind) direction. Box (left) shows important directions (interstellar wind vector, apex, α-Centauri) in the ecliptic plane.

transitions to a subsonic flow at the termination shock. There the kinetic energy of the supersonic flow is largely converted into thermal energy in the subsonic plasma beyond the shock. The subsonic heated postshock solar wind plasma (Fig. 2, top) flows in the heliospheric sheath around the termination shock and down the heliospheric tail, where it eventually mixes with the interstellar galactic plasma at distances > 5000 AU [10]. The galactic plasma (Fig. 2, bottom) flows around the heliopause, the boundary separating solar and galactic plasmas.

## 2. Three-dimensional heliosphere

Three fundamental factors make the heliosphere essentially asymmetric: (1) the motion of the Sun with respect to the surrounding interstellar medium, sometimes described as the interstellar wind; (2) asymmetry of the solar wind flow in heliolatitude; and (3) interstellar magnetic field of the unknown magnitude and direction. The interstellar wind velocity and direction are well established: 26 km/s (or 5.2 AU/yr) and ecliptic latitude  $\beta \approx 5^\circ$  and ecliptic longitude  $\lambda \approx 255^\circ$ , respectively. The solar wind flow is highly anisotropic during solar minimum [9,11] with the typical velocities near ecliptic 450 km/s and over the poles 750 km/s. The direction of interstellar magnetic field in the Sun's vicinity is unknown. It is anticipated that the shapes of both the heliopause and the termina-

tion shock will reveal the asymmetry of the magnetic field, with the stronger effect expected in case of the heliopause.

Voyager 1 will be turned off in 2020–2025 at 150 AU from the Sun because of the decreasing power provided by its radioisotope thermoelectric generators. If operational when the spacecraft reaches the heliopause, Voyager 1 will not be able to determine the shape of the heliosphere or the heliopause and the directional variations of the nature of the heliospheric sheath or the processes therein. The spacecraft probes the essentially asymmetric three-dimensional heliospheric boundary in one point-direction as the future Interstellar Probe will do. Interstellar Probe will reach 300–400 AU from the Sun in the approximately same direction as Voyager 1 [12–14].

Our present experimental capabilities to explore in situ the outer heliosphere are limited by the technical difficulties, including propulsion limitations, and budgetary realities of sending space probes to this distant region and beyond. At the same time, the structure and the physical processes at the solar system galactic frontier—the heliospheric interface—are of fundamental importance for understanding the interaction of our star, the Sun, with the galactic medium. This region also needs to be charted for optimizing our first foray into interstellar space by the Interstellar Probe mission and for supporting the truly interstellar exploration and interstellar travel of the future.

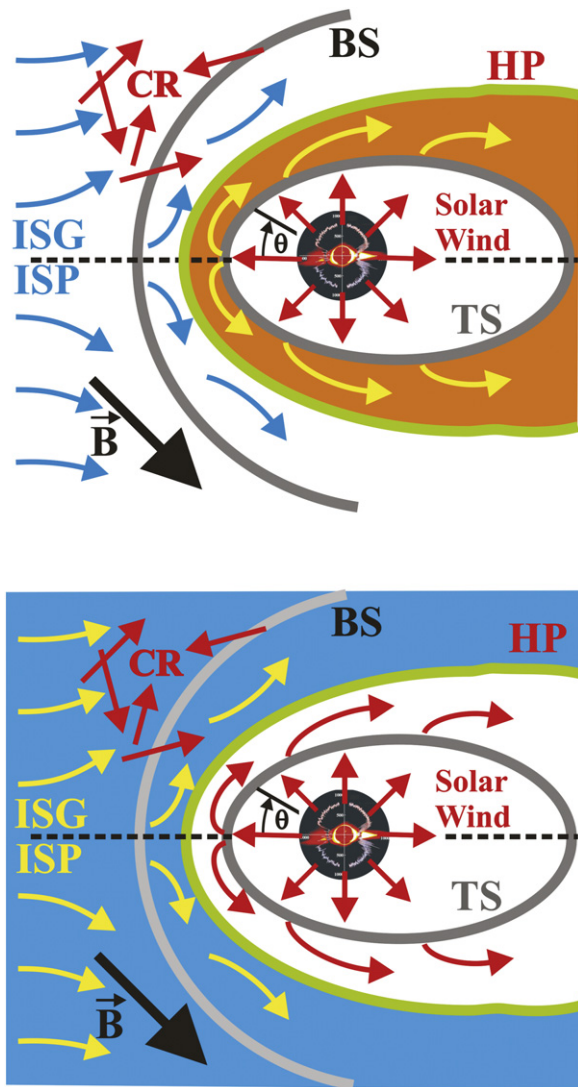


Fig. 2. Interaction of the solar wind with the interstellar medium. ISG(P)—interstellar gas (plasma); BS—bow shock; TS—termination shock; HP—heliopause; CR—cosmic rays; B—magnetic field. Asymmetry of Sun’s output pattern [9] illustrates conditions typical for solar minimum. Angle  $\theta$  is counted from the upwind (interstellar wind) direction. Top: The heliospheric sheath (heliosheath) region (orange; between TS and HP) contains the heated postshock solar wind plasma and pickup protons, a source of heliospheric energetic neutral atoms (ENAs); IBEX (launch in 2008) will image this region in fluxes of ENAs. Bottom: Interstellar plasma (blue) flows around the heliopause. Imaging in extreme ultraviolet (EUV) will probe this flow and map the heliopause as discussed in this work.

### 3. Remote sensing

Clearly, only remote techniques, supported and validated by the “ground-truth” in situ measurements by Voyagers 1 and 2 and Interstellar Probe, will enable a

comprehensive exploration and “putting on the maps” the solar system galactic frontier. The sheer size of the heliosphere calls for remote techniques to probe its global time-varying three-dimensional properties [15–17].

Two most promising experimental concepts have emerged to remotely study the heliospheric interface. These concepts rely on emissions originating at the solar system galactic frontier and reaching the observer at 1 AU with little disturbance. First, heliosphere imaging in fluxes of energetic neutral atoms (ENAs) will probe the plasma properties in the heliospheric sheath between the termination shock and the heliopause (Fig. 2). Second, imaging of the heliosphere in extreme ultraviolet (EUV) with high spectral resolution will map the heliopause.

The concept of ENA imaging of the heliospheric interface originated in late 1970s and early 1980s [18,19]. (Some not readily available publications can be downloaded from <http://astronauticsnow.com/ENA/>.) The first dedicated space experiment and instrumentation to detect ENAs from the heliospheric interface had been prepared for launch by mid-1980s. The mission was repeatedly delayed and the experiment faded away [15,19].

In 1992, a prediction of strong anisotropy of heliospheric ENA fluxes pointed to ENA imaging as a promising tool of studying the heliospheric sheath [20]. Today, the concept [21] and the new generation of ENA instrumentation [15,22,23] are mature. NASA’s Interstellar Boundary Explorer [23] (IBEX) will be launched in 2008 to perform heliosphere ENA imaging. Global ENA images would clearly differentiate [21] between physically distinct possibilities of processes at the termination shock and beyond and reveal properties of the plasma and pickup protons in the heliospheric sheath. IBEX will deploy in a highly eccentric orbit, with a Sun-pointed spinning spacecraft obtaining all-sky ENA images in several energy bins each six months [23].

The second concept to map the heliopause in EUV and to explore the flow of interstellar plasma around it (Fig. 2, bottom) was formulated in 1990s [17,24,25]. EUV imaging is the next logical step [17,26,27] in remote probing of the solar system galactic frontier after IBEX will have examined the termination shock and imaged the plasma and pickup protons in the heliospheric sheath in fluxes of ENAs. EUV imaging will build upon IBEX advances, leading to a comprehensive exploration of the complex interaction of the Sun with the surrounding interstellar medium.

We originally proposed to map the heliopause in the resonance line of the singly charged oxygen ion,  $O^+$ , at

83.4 nm [17,24,25]. The concept has evolved however and the most promising spectral line for such an experiment is believed to be the resonance line of the singly charged helium ion,  $\text{He}^+$ , 30.378 nm [16,17,26,27]. This line is often referred to as the 30.4-nm (304-A) line. EUV imaging of the global heliosphere requires advancing the instrumentation state-of-the-art by a factor of 100, which is being pursued [27,28].

#### 4. Heliosphere in EUV

Three main sources contribute to radiation fluxes at 30.4-nm, the spectral band of interest, in the heliosphere: the glow of interstellar plasma and pickup ions; galactic emissions (stars and hot plasmas in the Local Bubble); and emissions of the solar wind. Measurements of the glow of interstellar plasma open a way for mapping the heliopause. The pickup ion glow and solar wind emissions present the foreground radiation at this wavelength and galactic emissions are the background. The specifics of the new instrumentation concept would allow separation and simultaneous measurement of these three sources of radiation [27,28].

Two most abundant ions in interstellar plasma are singly charged helium  $\text{He}^+$  and oxygen  $\text{O}^+$  ions, with the corresponding resonance spectral lines at 30.4 and 83.4 nm, respectively. (Protons cannot be imaged optically at all; in contrast, the way to image proton populations is by measuring fluxes of ENAs [15]. Interstellar neutral atoms are unsuitable for heliopause mapping in UV/EUV because they penetrate deep into the heliosphere. Most of the glow of heliospheric neutrals, as seen by an observer near 1 AU, would originate within the 15-AU region.)

Expected radiance of the interstellar plasma ion glow is in the milli-Rayleigh range for helium and the micro-Rayleigh range for oxygen [16,17,24–27]. (1 Rayleigh = 1 R =  $10^3$  mR =  $10^6$   $\mu$ R =  $10^6/4\pi$  phot/cm<sup>2</sup> sr<sup>-1</sup> s<sup>-1</sup>.) Radiance of 1 mR is a flux of one photon per square centimeter per second from a solid angle of  $6.4^\circ \times 6.4^\circ$ . Measurement of milli-Rayleigh radiances with a high spectral resolution already presents a major instrumental challenge, and obtaining sky maps in the micro-Rayleigh range is presently unrealistic [16,26–28]. Therefore, we will concentrate exclusively on radiation at the  $\text{He}^+$  resonance line of 30.4 nm.

##### 4.1. Heliopause moat

The heliopause [5–8] separates the interstellar and solar wind plasmas (Fig. 2). Fig. 3 illustrates a typical

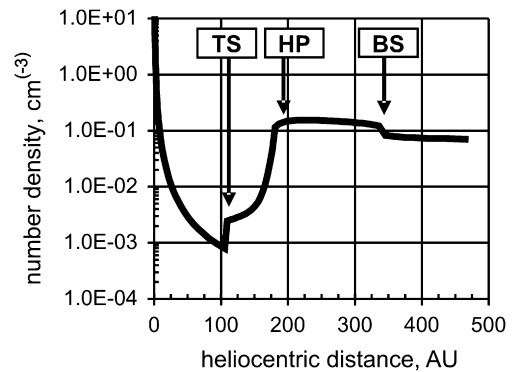


Fig. 3. Typical plasma number density variation with the heliocentric distance in the upwind direction [17]. The arrows indicate the positions of the termination shock (TS), heliopause (HP), and bow shock (BS). The plasma number density changes one–two orders of magnitude across the heliopause.

heliocentric variations of the plasma number density in the approximately upwind direction (with respect to the interstellar wind). The plasma density rapidly decreases with the expansion of the solar wind. Interstellar plasma cannot cross the heliopause and flows around it, resulting in a number density change of one–two orders of magnitude across the heliopause. One can thus imagine the Sun surrounded by an interstellar ion “wall” beyond an empty cavity, the “heliopause moat,” limited by the heliopause boundary. We do not know whether the heliopause is stable under such conditions.

##### 4.2. Heliopause mapping

This heliopause moat suggests a way of remote, from 1 AU, mapping of the heliopause. Singly charged interstellar  $\text{He}^+$  ions beyond the heliopause would scatter solar emissions in the ion resonance line. The solar 30.4-nm line (Fig. 4) is well characterized [29] and it is being monitored by spacecraft [30]. The Sun’s emission at 30.4 nm is not exactly isotropic [31] which would need to be accounted for. Measurements of the scattered solar radiation, the LISM plasma glow, would open an access to the heliopause and the region beyond.

For an observer at  $R_E = 1$  AU looking in the antisolar direction, glow radiance  $F(\theta)$  (photon/cm<sup>2</sup> s<sup>-1</sup> sr<sup>-1</sup>) is an integral along the line of sight

$$F(\theta) = \frac{1}{4\pi} \int_{R_E}^{\infty} N_{\text{I}^+}(R, \theta) g_{\text{I}}(R) dR,$$

where the  $g$ -factor (scattering rate per ion per second)  $g_{\text{I}}(R)$  depends on the distance from the Sun,  $N_{\text{I}^+}(R, \theta)$

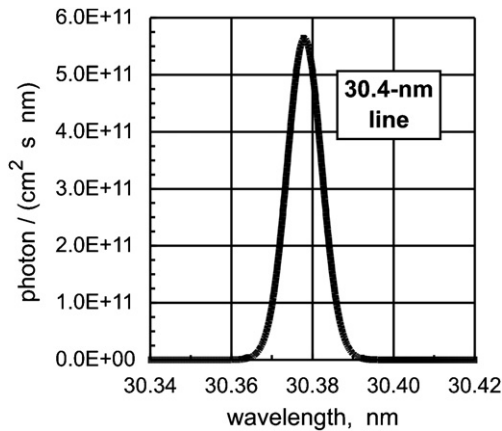


Fig. 4. Typical solar line at 30.4 nm.

is the local ion number density, and the scattering phase function is assumed isotropic [17].

For a simplified case of (1) vanishing ion number density inside the heliopause ( $R < R_{HP}$ ) and (2) interstellar plasma (beyond the heliopause) at rest with a uniform number density and constant temperature, the radiance would be

$$F(\theta) = \frac{N_{I+g_{I,E}} R_E^2}{4\pi} \frac{1}{R_{HP}},$$

where  $g_{I,E}$  is the  $g$ -factor at 1 AU. The sky brightness is thus inversely proportional to the distance to the heliopause in the direction of observation. Measuring the directional dependence (imaging) of the interstellar plasma glow will map and reveal asymmetry of the heliopause. The detailed temperature, velocity, and number density flow fields of the LISM plasma are needed for accurate treatment of the problem, and the  $g$ -factors should be calculated for the specific local velocity distribution functions of the ions [17].

The glow of  $\text{He}^+$  ions in the solar wind would produce the foreground radiation. These ions are produced by ionization of interstellar neutrals penetrating the heliosphere. The newly formed ions are picked up by the solar wind flow and carried to the termination shock as the pickup ions [32–35]. The pickup ions are singly charged and characterized by a spherical shell velocity distribution function. The glow of the pickup ions is the line radiation spectrally similar to the LISM plasma glow.

Fig. 5 shows the calculated radiance of the glow of the LISM plasma beyond the heliopause and the glow of the pickup ions; the ion-to-neutral ratio for helium is assumed to be 0.3125 in the LISM. (The detailed model is described elsewhere [17]). The initial slight increase

of the LISM plasma brightness with the angle  $\theta$  is due to the Doppler effect as the galactic plasma velocity radial component diminishes in the plasma turning around the heliopause. The glow falls as the heliopause moves away from the Sun and the Doppler effect reduces the  $g$ -factor.

The brightness of the interstellar plasma glow is roughly proportional to the number density of the interstellar gas ionized component, while the pickup ion glow is roughly proportional to the number density of the neutral component. Therefore, by measuring the upwind-to-downwind brightness ratio one would establish the ionization state of helium in the interstellar medium in the Sun's vicinity.

### 4.3. Galactic emission background

The galactic EUV radiation background consists of the continuum and line radiation emitted by stars (stellar radiation field) and the radiation emitted by hot interstellar plasmas. The stellar radiation dominates the EUV continuum background at wavelengths larger than 20 nm [36,37], including the spectral region of interest at 30.4 nm. The stellar radiation field is a continuum with negligible line emissions.

Based on the most complete database obtained by the Extreme Ultraviolet Explorer (EUVE), the total (at least 90% complete) radiation field is  $13.5 \text{ phot/cm}^2 \text{ s}^{-1} \text{ nm}^{-1}$  around 30 nm [36]. If one assumes isotropic background, then this stellar radiation field translates into the  $1.3 \times 10^{-2} \text{ mR/nm}$  spectral radiance [16,17]. (The predicted continuum radiation from the Local Bubble plasma,  $6.7 \times 10^{-4} \text{ mR/nm}$ , is significantly weaker [16,17].) The stellar radiation is highly anisotropic, however. Two white dwarfs, G191-2B2 ( $\lambda = 80.6^\circ$  and  $\beta = +29.8^\circ$ ) and Feige 24 ( $\lambda = 37.6^\circ$  and  $\beta = -10.9^\circ$ ), dominate the background at 30.4 nm [36]. For directions away from these two bright sources the stellar continuum background would be significantly smaller.

Fig. 6 illustrates our galactic environment. The Sun is embedded in a small, several parsec long, and relatively dense ( $0.1 \text{ cm}^{-3}$ ) local interstellar cloud, sometimes called the local fluff [38–40]. The cloud is too cold (7000–8000 K) to emit EUV radiation, but it is surrounded by a region filled with hot ( $\sim 10^6 \text{ K}$ ) and rarefied ( $\sim 0.005 \text{ cm}^{-3}$ ) plasmas, the Local Bubble. The Local Bubble may extend up to 200 pc in some directions and even expand into the galactic halo [41]. The hot plasmas have probably been heated by nearby supernovae with the resulting deviations from the thermodynamic equilibrium and cosmic abundances [42]. We

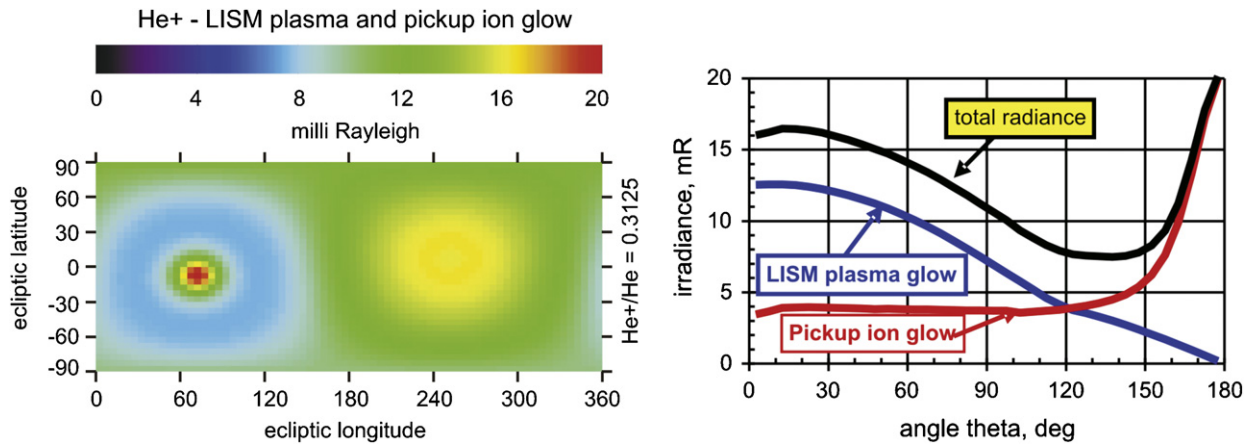


Fig. 5. Left: Simulated all-sky map (Mercator projection in ecliptic coordinates) of the LISM plasma glow (“heliopause glow”) and the solar wind pickup ion glow at 30.4 nm. A broad bright area in the upwind direction is centered at 255° longitude. Pickup ion glow is concentrated in the downwind direction—a bright narrow region at 75° longitude. Right: LISM plasma glow and pickup ion glow as function of the angle  $\theta$  from the upwind direction. The upwind-to-downwind ratio of glow radiance depends on the ionization state of helium in the local interstellar medium.

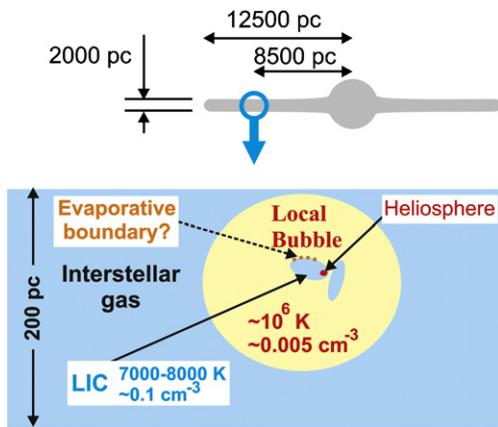


Fig. 6. The heliosphere, local interstellar cloud (LIC), Local Bubble, and the Galaxy.

used the standard model [43] to calculate the isotropic EUV background radiation due to the Local Bubble hot plasma [16,17]. Processes at the evaporative boundary of the local cloud [44] may also contribute to the EUV background; no experimental evidence of such radiation has been obtained yet and this possibility needs further investigation.

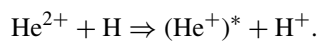
We note that recent measurements (on the Cosmic Hot Interstellar Plasma Spectrometer, or CHIPS, space mission) of diffuse emissions in the wavelength range of 9–26.5 nm suggest that the emissions of hot plasmas in the Local Bubble are significantly weaker than our present concepts predict [45]. If this important finding is confirmed, then the contribution of the Local Bubble

to the 30.4-nm background in the heliosphere would be smaller than assumed by us.

#### 4.4. Solar wind emission foreground

Charge-exchange collisions between the solar wind alpha particles ( $\text{He}^{2+}$  ions) and heliospheric atomic hydrogen would produce unique emissions at 30.4 nm [16]. Helium is the second most abundant component of the solar wind, with alpha particles constituting 2–5% of the number of plasma ions. Interstellar hydrogen atoms, the most abundant component of the neutral gas in the LISM, penetrate and fill the heliosphere, providing the background gas of atomic hydrogen for charge-exchange collisions. In addition, heliospheric ENAs could significantly contribute to a neutral hydrogen population in the immediate Sun’s vicinity [46].

The most efficient channel of charge exchange collisions [16] between alpha particles and hydrogen atoms (accidental resonant charge exchange) produces helium ions in the first excited state ( $2p$ ) or ( $2s$ )



The  $\text{He}^+(2p)$  ions would quickly (0.1 ns) decay to the ground state with the emission of a 30.378-nm photon. The emitting helium ion moves with the solar wind velocity, so the photon would correspondingly be Doppler-shifted. The efficiency of charge exchange strongly depends on the collision velocity, with the corresponding cross-section being 3.3 times higher for typical

velocities of the fast (polar) solar wind than for typical velocities of the slow (ecliptic) solar wind [16].

All-sky images of solar wind emissions would map the flow pattern (number density and velocity) of the three-dimensional solar wind everywhere in the heliosphere, including over the Sun’s poles. The areas in the sky with the high-speed solar wind would stand out in brightness because of the higher velocity-dependent charge-exchange cross sections. In addition, spectral analysis of Doppler-shifted 30.378-nm photons would directly establish the solar wind velocity in a given direction. A Doppler shift of 0.005 nm (0.05 Å) corresponds to a 50-km/s velocity.

Fig. 7 shows a simulated all-sky image of solar wind emissions at solar minimum [47]. The effective solar magnetic dipole is tilted by the angle  $\lambda_M$  with respect to the Sun’s spin axes. (The Sun spin axis is tilted 7.25° from the normal to the ecliptic plane.) The slow solar wind is confined within the  $\pm\tau_0$  angle from the magnetic equator. The simulated map of total solar wind emissions and spectrally resolved Doppler-shifted images [47] clearly show that heliosphere imaging would be able to determine [47] the angle  $\xi_0 = \tau_0 + \lambda_M$  (defining the region with the mixed fast and slow solar wind flows, see Fig. 7, middle) but would not separate angles  $\tau_0$  and  $\lambda_M$ . These angles could perhaps be separated with the help of other complementary observations.

Accumulation of an all-sky image would require at least one–two weeks of observations [27] washing out many flow features in the near equatorial region. In addition, most of the solar wind emissions contributing to the observed radiance from a given direction are produced (the source function) within 10–25 AU from the Sun. Depending on the solar wind velocity and direction of observation, such distances correspond to time intervals from one to four Sun’s rotations. In other words, the solar wind plasma contributing to the observed emissions from a given direction originates from the regions on the Sun surface with different solar longitudes averaged over from one to four Sun’s rotations.

Consequently, a realistic space experiment should focus on measuring the angle  $\xi_0$  and its slow variation through the 11-year solar cycle. Therefore, one would require obtaining a few all-sky images per year. Measuring weak background photon fluxes is especially difficult for directions close to the Sun. Alternatively, one can instead periodically obtain an image of a one-pixel-wide (or, a few-pixel-wide) swath in the sky, from south to north ( $\pm 90^\circ$ ), in the antisolar direction. Fig. 8 shows spectral radiance for such a swath with high spectral resolution, revealing velocities of the solar wind flow from measured Doppler shifts. A swath

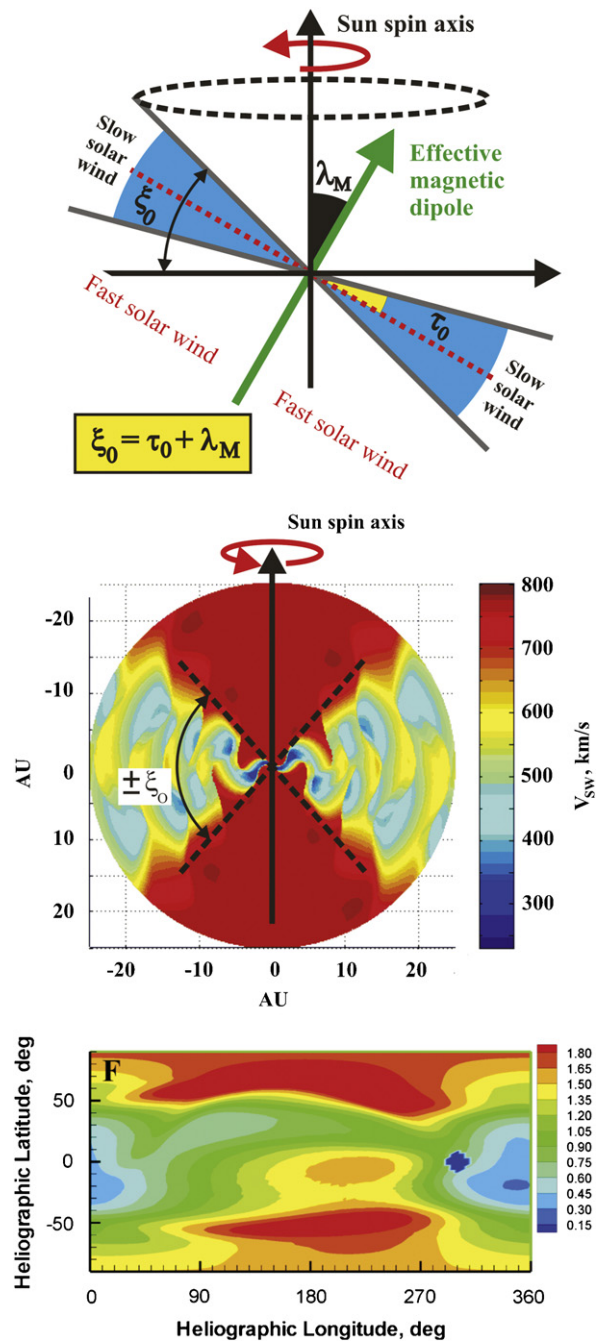


Fig. 7. Top: Model of the solar wind flow at solar minimum with the effective sun’s magnetic dipole tilted by the angle  $\lambda_M$  with respect to the Sun’s spin axes. The slow solar wind is confined with the  $\pm\tau_0$  angle from the magnetic equator. Middle: Solar wind velocity flow field. Bottom: A simulated all-sky image (Mercator projection) of the solar wind emissions (mR) at 30.4 nm. Details of the model, calculations, and more images can be found elsewhere [47].

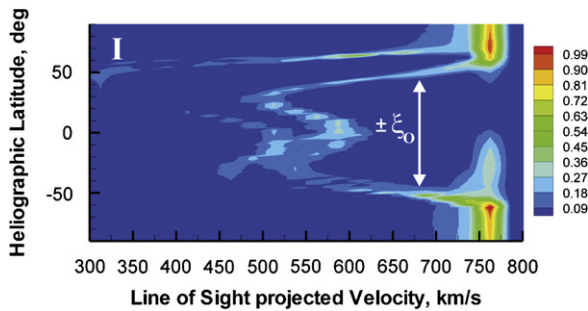


Fig. 8. Spectral radiance (mR/0.005 nm) for a swath in the sky (latitudes from  $-90^\circ$  to  $+90^\circ$  in the anti-solar direction with the corresponding (derived from Doppler shifts) velocities shown along the horizontal axis [46].

image can be accumulated in a couple days [27]. Swath observations would always image the solar wind passing the Earth's vicinity, relating them to simultaneous complementary in-situ solar wind measurements by near-Earth spacecraft. In addition, the instrument would always be pointed at least  $90^\circ$  away from the direction toward the Sun, thus significantly simplifying the baffle system.

Since the Sun rotates, one-dimensional south–north swath observations during one rotation of the Sun ( $\sim 27$  days as observed from the Earth moving around the Sun) would allow inferring the three-dimensional flow field of the solar wind in the entire heliosphere. Simultaneously, the global image of the heliopause (heliopause map) would be obtained in one year, as the Earth moves around the Sun and the south–north swaths cover the entire  $4\pi$  sky. This mapping frequency meets the requirement for imaging and mapping the heliopause [16,17,27].

#### 4.5. Spectral radiance

Fig. 9 shows representative spectral radiance (at 1 AU) of the three main radiation sources at 30.4 nm: glow of the interstellar plasma (heliopause glow) and of the pick up ions (foreground), solar wind emission foreground, and Local Bubble emission background. An instrument with a spectral resolution of 0.005 nm (0.05 Å), which corresponds (Doppler shifts) to a velocity difference of 50 km/s, would be able to separate the ion glow from solar wind emissions and interstellar emission lines.

### 5. Instrumentation challenge

The science objectives translate into the following performance characteristics of the instrumentation.

#### 5.1. Spectral resolution

A spectral resolution of 0.005 nm would reliably separate major sources (ion glow, solar wind emissions, Local Bubble emissions) of radiation at 30.4 nm, unambiguously reveal major details of the solar wind flow, directly measure the flow velocities with a 50-km/s accuracy, map the heliopause with high precision, and accurately identify emission lines (within the instrument spectral band) of hot plasmas in the Local Bubble.

#### 5.2. Spectral band

The new instrumentation concept favors a rather wide spectral range, almost 4-nm wide, centered on 30.4 nm [27,28]. This band can be further increased for study of Local Bubble plasmas.

#### 5.3. Angular resolution

A nominal  $5^\circ \times 5^\circ$  angular resolution in heliospheric images would meet the requirements of mapping the heliopause and imaging the three-dimensional solar wind flow [16,17,27].

#### 5.4. Sensitivity

Obtaining one one-dimensional south–north swath in the sky every couple days would correspond to an exposure time of 10,000–20,000 s/pixel (3–5.5 h/pixel).

#### 5.5. Instrumentation

Both the required sensitivity and the required spectral resolution calls for a roughly two-orders-of-magnitude improvement in performance characteristics compared to the state of the art of diffuse EUV radiation spectrometry [26–28]. Such advancement in instrumentation obviously presents a major challenge. The magnitude of this challenge, however, is not very different from the (successfully met) challenge of developing instrumentation for detection of ENAs in late 1970s and early 1980s [15,18].

A recent feasibility study showed that the desired instrument performance characteristics could possibly be achieved by combining multiple entrance slits with an optimized spectrometer design [27]. The new blur-free shape of the entrance slits was invented and tested [28] which opened a way of combining multiple slits in coded-aperture patterns. Computer simulations supported by experimental validation of key technologies

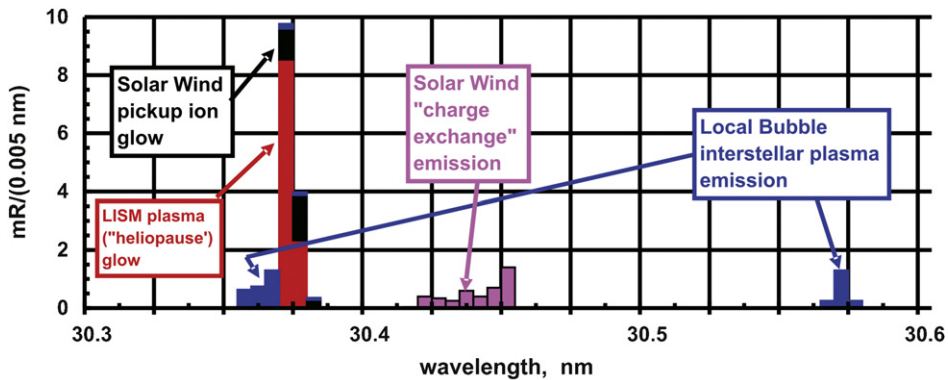


Fig. 9. Representative spectral radiance (at 1 AU) at 30.4 nm summed over 0.005-nm bins for a typical observational direction. The radiation combines contributions from the glow of interstellar plasma (heliopause glow) and the pick up ions glow foreground, solar wind emission foreground, and Local Bubble emission background.

have confirmed promising capabilities of the new instrumental concept. Detailed discussion of the instrumentation is presented elsewhere [27,28].

## 6. Space mission and experiment

Global imaging of the heliosphere at 30.4 nm will (1) map the heliopause and probe the ionization state of the LISM and asymmetry of the magnetic field of the nearby interstellar medium; (2) reveal the time-varying three-dimensional properties (number densities and velocities) of the solar wind, including the flow properties in the regions over the Sun's poles; and (3) measure line emissions of hot plasmas in the Local Bubble. This space experiment will contribute to meeting science objectives of two major areas of NASA Science Directorate, study of the Sun–Earth System (former Sun–Earth Connections Division) and Universe (Astrophysics Division).

Measurements of very low photon fluxes require minimal detector noise. Therefore, the spacecraft must be placed in an orbit outside the magnetosphere of the Earth and outside the geocorona. Spacecraft in high-apogee Earth orbits satisfy such requirements when close to apogee. The observations however are interrupted during the perigee passes which also expose the spacecraft and instrumentation to high fluxes of energetic particles in the radiation belts. Mission requirements of NASA's IBEX [23] are conceptually similar to those of heliosphere imaging in EUV: the spacecraft maps the heliosphere in weak ENA fluxes. The IBEX spacecraft will be deployed in a high-apogee orbit using a small launcher (Pegasus), with the mission costs capped by the limits of the Small Explorer (SMEX) program.

An interplanetary platform would provide perfectly quiet observational conditions for heliosphere EUV imaging but it requires high delta-V launch capabilities for deployment and large ground antennas for communications with the spacecraft and thus expensive operations. Such requirements consequently drive the cost up, making a space mission to image the heliosphere in EUV less competitive for limited funds in NASA.

EUV imaging of the heliosphere can also be conducted from the lunar surface. Observations from a lunar surface site would first require investigations of the effects of possible glow at 30.4 nm in the near-Moon environment and possible effects of lunar dust on the instrumentation and on observations.

Our mission concept to image the heliosphere in EUV combines advantages of quiet environment of an interplanetary mission, a relatively low delta-V of a high-apogee Earth-orbiting mission, a straightforward spacecraft design, and simplicity and low cost of mission operations and control. While the mission is still more costly than what can be realistically done within the SMEX program, it would fit into the cost limits of the Medium Explorer (MIDEX) program with the cost significantly smaller than the MIDEX cap.

We propose to deploy a spacecraft in a libration point, L3, L4, or L5, of the Earth–Moon system (Fig. 10). In the rotating Earth–Moon reference frame, there are five points—L1, L2, L3, L4, L5—of gravitational equilibrium (under the assumption of vanishing Sun's gravity). All points are in the plane of the Moon orbit around the Earth. Libration points L4 and L5 form equilateral triangles with the Earth and the Moon as shown in Fig. 10. These two points are inherently stable—a body (spacecraft) placed in L4 or L5 would stay in these points (in the Earth–Moon rotating reference frame) indefinitely.

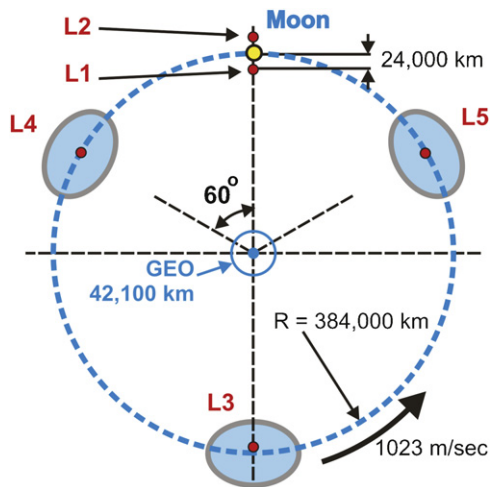


Fig. 10. Earth–Moon libration points L3, L4, and L5 offer excellent locations (light-blue areas) for deploying a spacecraft to conduct heliosphere imaging in EUV.

Sun's gravity disturbs this ideal case, so the spacecraft would move around these libration points in an open halo orbit. What is important for our purposes is that the spacecraft would stay in the approximate vicinity of a libration point outside the magnetosphere, requiring minimal delta-V (several m/s) for station-keeping for a mission lasting several years.

Spacecraft deployment to the Earth–Moon L4 and L5 points can be efficiently achieved using lunar gravity assist. The transfer from a low-earth parking orbit would require delta-V less than 3.3 km/s, including about 3.1 km/s for the initial boost from the parking orbit, 0.1 km/s for midcourse maneuvers with a very generous margin, and 0.1 km/s for phasing into the libration-point station. Note that this delta-V is significantly smaller than the velocity increment required for placing a spacecraft into geostationary orbit (GEO), 4.2 km/s for a Cape-Canaveral-launched spacecraft. Libration points L4 and L5 attracted space visionaries and enthusiasts (e.g., “L5 Society” of 1970s) for many years as possible locations for space stations and space colonies, but they have never been used for scientific spacecraft.

The conditions at L4 or L5 are favorable for a mission to image the heliosphere in EUV. The spacecraft would be at the distance of  $\sim 384,000$  km from the Earth, well beyond the geocorona and the magnetosphere and with observations uninterrupted by eclipses. The absence of eclipses would also significantly simplify spacecraft design, especially its thermal control and electric power subsystems. Minimal environmental

torques simplify the spacecraft attitude control system. A relatively short (compared to interplanetary missions) distance to the spacecraft makes communications easy. A small 5-W spacecraft transmitter can readily provide a 10-kb/s communication link for a 1.5 m ground antenna. In addition, the spacecraft would slowly move in the sky, making its tracking easy and allowing long uninterrupted access (up to 10 h) from the same location on the ground.

Scanning pixel-wide south–north swaths in the antisolar directions seems to be the most promising approach for achieving science goals of heliosphere EUV imaging. We note that observations would be impossible in directions close to those toward the Earth or the Moon. This constraint may reduce the effective available observation time by one quarter. (On the other hand, measurements of 30.4-nm emissions from the near-Earth region would be valuable for studying the plasmasphere and magnetosphere.) Deployment of the spacecraft in the Earth–Moon libration point L3 could significantly reduce this time loss because the Earth and the Moon are always aligned in the same direction as seen from L3.

(We note that the libration point L2 of the Sun–Earth system—about 1.5 million km away from the Earth in the antisolar direction—would also be an excellent location for a spacecraft to image the heliosphere in EUV. The spacecraft would be free of the interfering effects of the Earth or the Moon, with the perfect 100% observation duty cycle. Such a mission would require however larger delta-V and communications capabilities.)

The EUV spectrometer for heliosphere imaging will be fixed with respect to the spacecraft, with its pointing achieved by controlling attitude of the spacecraft. Since heliospheric polar regions would be observed during each south–north scan, the dwell time in directions with different latitudes could be optimized to achieve a uniform duty cycle (observation time) coverage of the whole sky. This adjustment is especially important for observations close to the ecliptic plane. Continuous coverage of the polar regions would also provide an opportunity for monitoring instrument detection efficiency (observing constant Local Bubble emissions) and validating consistency of accounting for variations of the solar 30.4-nm line.

## 7. Conclusions

Remote sensing of the solar system galactic frontier is of fundamental importance for understanding the interaction of our star, the Sun, with the surrounding galactic medium and for supporting the truly interstellar

exploration and interstellar travel of the future. The NASA's IBEX mission will image the heliospheric sheath in ENA fluxes and revolutionize our understanding of the termination shock and the processes beyond. Mapping of the heliopause in EUV is the next logical step in remote exploration of the galactic frontier. Heliosphere imaging at 30.4 nm with ultrahigh spectral resolution will open a new window on the structure of and the processes at the heliopause and beyond. The science objectives have been translated into requirements to the instrumentation. Feasibility studies have shown that these requirements could be met by a new instrumentation concept presently under development. The mission and spacecraft design do not present special difficulties and can be optimized when realistic performance characteristics of the instrumentation are firmed up. The space mission to image the heliosphere in EUV can be accomplished within the cost of a MIDEX mission.

## Acknowledgment

This work was supported in part by a NASA grant.

## References

- [1] L. Davis Jr., Interplanetary magnetic fields and cosmic rays, *Physical Review* 100 (1955) 1440–1444.
- [2] E.N. Parker, *Interplanetary Dynamical Processes*, Wiley-Interscience, New York, 1963.
- [3] A.J. Dessler, Solar wind and interplanetary magnetic field, *Reviews of Geophysics* 5 (1967) 1–41.
- [4] W.I. Axford, The interaction of the solar wind with the interstellar medium, *Solar Wind*, vol. SP-308, NASA Special Publication, 1972, pp. 609–660.
- [5] V.B. Baranov, Gasdynamics of the solar wind interaction with the interstellar medium, *Space Science Reviews* 52 (1990) 89–120.
- [6] S.T. Suess, The heliopause, *Reviews of Geophysics* 28 (1990) 97–115.
- [7] H.J. Fahr, H. Fichtner, Physical reasons and consequences of a three-dimensionally structured heliosphere, *Space Science Reviews* 58 (1991) 193–258.
- [8] G.P. Zank, Interaction of the solar wind with the local interstellar medium: a theoretical perspective, *Space Science Reviews* 89 (1999) 1–275.
- [9] D.J. McComas, H.A. Elliott, N.A. Schwadron, J.T. Gosling, R.M. Skoug, B.E. Goldstein, The three-dimensional solar wind around solar maximum, *Geophysical Research Letters* 30 (10) (2003), doi: 10.1029/2003GL017136.
- [10] S. Jaeger, H.J. Fahr, The heliospheric plasma tail under influence of charge exchange processes with interstellar H-atoms, *Solar Physics* 178 (1998) 631–656.
- [11] M. Neugebauer, The three-dimensional solar wind at solar activity minimum, *Reviews of Geophysics* 37 (1999) 107–126.
- [12] P.C. Liewer, R.A. Mewaldt, J.A. Ayon, R.A. Wallace, NASA's interstellar probe mission, in: *STAIF-2000 Proceedings*, 2000.
- [13] M. Gruntman, Instrumentation for interstellar exploration, *Advances in Space Research* 34 (2004) 204–212.
- [14] M. Gruntman, R.L. McNutt Jr., R.E. Gold, S.M. Krimigis, E.C. Roelof, J.C. Leary, G. Gloeckler, P.L. Koehn, W.S. Kurth, S.R. Oleson, D. Fiehler, Innovative Explorer mission to interstellar space, *Journal of British Interplanetary Society* 59 (2) (2006) 71–75.
- [15] M. Gruntman, Energetic neutral atom imaging of space plasmas, *Review of Scientific Instruments* 68 (1997) 3617–3656.
- [16] M. Gruntman, Imaging the three-dimensional solar wind, *Journal of Geophysical Research* 106 (2001) 8205–8216.
- [17] M. Gruntman, Mapping the heliopause in EUV, in: *The Outer Heliosphere: The Next Frontiers*, Pergamon, 2001, pp. 263–271.
- [18] M. Gruntman, V.B. Leonas, Neutral solar wind: possibilities of experimental investigation, Report (Preprint) 825, Space Research Institute (IKI) Academy of Sciences, Moscow, 1983. (This and some other early publications can be downloaded from (<http://astronauticsnow.com/ENA/>.)
- [19] M. Gruntman, V.B. Leonas, S. Grzedzielski, Neutral solar wind experiment, in: *Physics of the Outer Heliosphere*, Pergamon Press, New York, 1990, pp. 355–358.
- [20] M.A. Gruntman, Anisotropy of the energetic neutral atom flux in the heliosphere, *Planetary and Space Science* 40 (1992) 439–445.
- [21] M. Gruntman, E.C. Roelof, D.G. Mitchell, H.J. Fahr, H.O. Funsten, D.J. McComas, Energetic neutral atom imaging of the heliospheric boundary region, *Journal of Geophysical Research* 106 (2001) 113–154.
- [22] C.J. Pollock, K. Asamura, J. Balonado, M.M. Balkey, P. Barker, J.L. Burch, E.J. Korpela, J. Cravens, G. Dirks, M.-C. Fok, H.O. Funsten, M. Grande, M. Gruntman, J. Hanley, J.-M. Jahn, M. Jenkins, M. Lampton, M. Marckwordt, D.J. McComas, T. Mukai, G. Penegor, S. Pope, S. Ritzau, M.L. Schattenburg, E. Scime, R. Skoug, W. Spurgeon, T. Stecklein, S. Storms, C. Urdiales, P. Valek, J.T.M. van Beek, S.E. Weidner, M. Wuest, M.K. Young, C. Zinsmeyer, Medium energy neutral atom (MENA) imager for the IMAGE mission, *Space Science Reviews* 91 (2000) 113–154.
- [23] D. McComas, F. Allegrini, P. Bochsler, M. Bzowski, M. Collier, H. Fahr, H. Fichtner, P. Frisch, H. Funsten, S. Fuselier, G. Gloeckler, M. Gruntman, V. Izmodenov, P. Knappenberger, M. Lee, S. Livi, D. Mitchell, E. Moebius, T. Moore, D. Reisenfeld, E. Roelof, N. Schwadron, M. Wieser, M. Witte, P. Wurz, G. Zank, The Interstellar Boundary Explorer (IBEX), in: *Physics of the Outer Heliosphere*, AIP Conference Proceedings, vol. 719, American Institute of Physics, Melville, NY, 2004, pp. 162–181.
- [24] M. Gruntman, H.J. Fahr, Access to the heliospheric boundary: EUV-echoes from the heliopause, *Geophysical Research Letters* 25 (1998) 1261–1264.
- [25] M. Gruntman, H.J. Fahr, Heliopause imaging in EUV: Oxygen O<sup>+</sup> ion 83.4-nm resonance line emission, *Journal of Geophysical Research* 105 (2000) 5189–5200.
- [26] M. Gruntman, Solar system frontier: exploring the heliospheric interface from 1 AU, *Journal of British Interplanetary Society* 59 (2) (2006) 54–58.
- [27] M. Gruntman, M. Lampton, J. Edelman, Imaging three-dimensional heliosphere in EUV, in: S. Fineschi, R.A. Viereck (Eds.), *Solar Physics and Space Weather Instrumentation Proceedings of SPIE*, vol. 5901, SPIE-5901-3, 2005.
- [28] M. Lampton, J. Edelman, T. Miller, M. Gruntman, An EUV spectrometer for mapping the heliopause and solar wind, in:

- O.H.W. Siegmund (Ed.), UV, X-Ray, and Gamma-Ray Space Instrumentation for Astronomy XIV, Proceedings of SPIE, vol. 5898, SPIE-5898-36, 2005.
- [29] G.A. Doschek, W.E. Behring, U. Feldman, The widths of the solar He I and He II lines at 584, 537, and 304 Å, *Astrophysical Journal* 190 (1974) L141–L142.
- [30] D.L. Judge, D.R. McMullin, P. Gangopadhyay, H.S. Ogawa, F.M. Ipavich, A.B. Galvin, E. Möbius, P. Bochsler, P. Wurtz, M. Hilchenbach, H. Grünwaldt, D. Hovestadt, B. Klecker, F. Gliem, Space weather observations using the SOHO CELIAS complement of instruments, *Journal of Geophysical Research* 106 (2001) 26968–29963.
- [31] F. Auchère, J.W. Cook, J.S. Newmark, D.R. McMullin, R. von Steiger, M. Witte, The heliospheric He II 30.4 nm solar flux during Cycle 23, *Astrophysical Journal* 625 (2005) 1036–1044.
- [32] E. Möbius, D. Hovestadt, B. Klecker, M. Scholer, G. Gloeckler, Direct observation of He<sup>+</sup> pickup ions of interstellar origin in the solar wind, *Nature* 318 (1985) 426–429.
- [33] G. Gloeckler, The abundance of atomic 1H, 4He, and 3He in the local interstellar cloud from pickup ion observation on Ulysses, *Space Science Reviews* 78 (1996) 335–346.
- [34] E. Möbius, The local interstellar medium viewed through pickup ions recent results and future perspectives, *Space Science Reviews* 78 (1996) 375–386.
- [35] E. Möbius, D. Rucinski, M.A. Lee, P.A. Isenberg, Decreases in the antisunward flux of interstellar pickup He<sup>+</sup> associated with radial interplanetary magnetic field, *Journal of Geophysical Research* 103 (1998) 257–285.
- [36] J. Vallerga, The stellar extreme-ultraviolet radiation field, *Astrophysical Journal* 497 (1988) 921–927.
- [37] K.-P. Cheng, F.C. Bruhweiler, Ionization processes in the local interstellar medium: effects of the hot coronal substrate, *Astrophysical Journal* 364 (1990) 573–581.
- [38] R. Lallement, R. Ferlet, A.M. Lagrange, M. Lemoine, A. Vidal-Madjar, Local interstellar cloud structure from HST-GHRS, *Astronomy & Astrophysics* 304 (1995) 461–474.
- [39] P.C. Frisch, Characteristics of nearby interstellar medium, *Space Science Reviews* 72 (1995) 499–592.
- [40] J.L. Linsky, S. Redfield, B.E. Wood, N. Piskunov, The three-dimensional structure of the warm local interstellar medium. I. Methodology, *Astrophysical Journal* 528 (2000) 756–766.
- [41] B.Y. Welsh, D.M. Sfeir, M.M. Sirk, R. Lallement, EUV mapping of the local interstellar medium: the Local Chimney revealed?, *Astronomy & Astrophysics* 352 (1999) 308–316.
- [42] D.P. Cox, R.J. Reynolds, The local interstellar medium, *Annual Review Astronomy and Astrophysics* 25 (1987) 303–344.
- [43] M. Landini, B.C. Monsignori Fossi, The X-UV spectrum of thin plasmas, *Astronomy & Astrophysics Supplement Series* 82 (1990) 229–260.
- [44] J.D. Slavin, Consequences of a conductive boundary on the local cloud. I. No dust, *Astrophysical Journal* 346 (1989) 718–7272.
- [45] M. Hurwitz, T.P. Sasseen, M.M. Sirk, Observations of diffuse extreme-ultraviolet emissions with the Cosmic Hot Interstellar Plasma Spectrometer (CHIPS), *Astrophysical Journal* 623 (2005) 911–916.
- [46] M. Gruntman, V. Izmodenov, Mass transport in the heliosphere by energetic neutral atoms, *Journal of Geophysical Research* 109 (2004) A12108, doi: 10.1029/2004JA010727.
- [47] M. Gruntman, V. Izmodenov, V. Pizzo, Imaging the global solar wind flow in EUV, *Journal of Geophysical Research* 111 (2006) A04216.